The missing layer between the cloud hierarchy and massive star formation: direct mapping of the dense gas in W51 A

1 Scientific Justification

1.1 Scientific rationale:

Molecular clouds are hierarchical over a wide range of spatial scales, with smaller, denser structures embedded within larger, more diffuse ones[1]. While this organization is objectively captured by dendrogram analysis[2][3], how the nested structure relates to (massive) star formation remains contested: theories disagree on whether the gas reservoir for a massive star is confined to a single core (e.g., the turbulent-core model[4]) or is set by the larger-scale hierarchy (e.g., global hierarchical collapse[5]). We applied a dendrogram analysis uniformly to the ^{13}CO ($J = 1$–0) data of the FUGIN legacy survey[6] across 13 Galactic star-forming regions, and statistically compared the leaves—structures nested within the larger trunks—with isolated structures standing outside any hierarchy[7]; the active star-forming region W51 A, among the richest in both categories, exemplifies the classification (Figure 1a). Although the two span comparable spatial scales, the hierarchical environment selectively promotes massive star formation: the leaves harbor significantly more Hi-GAL clumps[8], the precursors of massive stars, than the isolated structures, with no excess in low-mass YSOs (Figure 1b).

The ^{13}CO ($J = 1$–0) line we used traces gas at $n \sim 10^3\,\mathrm{cm^{-3}}$, and even the optically thinner C^{18}O reaches only $n \sim 10^{3.5}\,\mathrm{cm^{-3}}$. Star formation, however, occurs only in dense gas above $n \gtrsim 10^4\,\mathrm{cm^{-3}}$[9]. For massive stars, the infrared luminosity tracing the star formation rate correlates linearly with the HCN luminosity tracing dense gas among Galactic massive star-forming clumps[10]: the activity is set by the dense gas the region has accumulated. The missing layer is thus the dense gas itself: it mediates the CO-traced reservoirs and the clumps they harbor, but is invisible to CO and reduced to a mere census by the clump catalog. Nor do existing data reach it: the only dense-gas mapping of W51 A, a Mopra 3-mm line survey[11] designed for cloud-averaged chemistry, has a $25' \times 30'$ field and $38''$ ($\sim$1 pc) beam that leave the isolated structures outside the map and the clump scale unresolved. Mapping this layer across the very structures we classified is therefore the necessary next step: it establishes whether the hierarchical environment indeed feeds massive star formation through the dense gas.

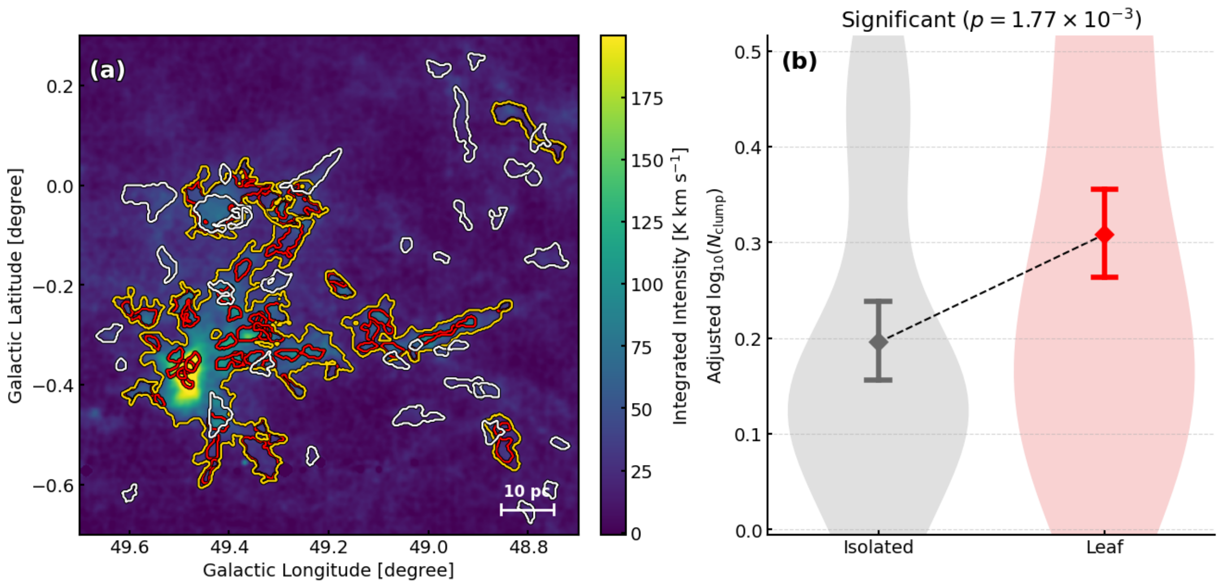

Figure 1: (a) ^{13}CO ($J = 1$–0) integrated intensity map of W51 A, the proposed target, overlaid with the dendrogram structures of our analysis[7]: trunks (gold), leaves (red), and isolated structures (white). (b) Number of associated Hi-GAL clumps per structure across the 13 regions, adjusted for the region-to-region variance: the leaves harbor significantly more clumps than the isolated structures, whereas the same analysis finds no significant difference in the YSO counts[7].

1.2 Immediate objective:

We propose to map the leaves and the isolated structures identified in W51 A in three dense-gas lines—HCN, HCO^+, and N_2H^+ (J=1–0)—established tracers of the gas at $n \gtrsim 10^4\,\mathrm{cm}^{-3}$ constituting the clumps[10][12], all covered in a single FOREST tuning (SAM45 spectral-window mode). This observation is the unique intermediate layer (Figure 2): it shares its observable, velocity-resolved line emission, with FUGIN and its scale, the clump, with Hi-GAL, whereas the two share neither, so the dense gas can be related to both within a single interpretive framework, from the reservoirs to the precursors.

First, we directly test whether the leaves indeed contain more dense gas than the isolated structures: their clump excess implies a corresponding excess in the dense gas itself, never measured beyond the CO-traced reservoirs. We require $\geq 5\sigma$ in the velocity-integrated HCN intensity of each structure. Undetected structures, most likely among the isolated ones, still yield upper limits on their dense-gas deficit, keeping the comparison conclusive. Spatially, the HCN distribution reveals whether the emission is concentrated at the catalogued clumps or extends beyond them, in which case the leaves store more raw material than the census indicates.

Second, we deepen the dynamical interpretation of the hierarchy, which our crossmatching could not address: with no observable shared between the CO data and the dust-derived catalog, and no velocity information in the latter, their correspondence has rested on positional coincidence in projection alone. The optically thin N_2H^+ gives the systemic velocity of each structure, required to $\lesssim 0.5\,\mathrm{km\,s^{-1}}$ on the $0.65\,\mathrm{km\,s^{-1}}$ velocity grid of the FUGIN cube (recorded at the 122.07 kHz channel spacing of SAM45), i.e., $\geq 3\sigma$ per channel at the line peak of each structure-averaged spectrum; whether the dense gas shares the velocity component of its host CO structure tests the physical coherence of the CO-defined hierarchy. Against that reference, the asymmetry of the optically thick HCO^+ profile diagnoses infall onto each structure[13], testing whether the leaves are still fed by the surrounding reservoir.

We map the full $1^\circ \times 1^\circ$ field in eight ≈81-min passes per scan direction: each pass covers the whole field with a coarse $48''$ row spacing (the $60'$ scans at $122''\,\mathrm{s^{-1}}$ requiring the 0.04 s dump time), with an OFF every ≈60 s and pointing checks between passes. Successive passes are offset in bisection order and alternate between the two orthogonal directions, building up the final $6''$ sampling while keeping the map uniform—only coarser—under weather loss or a reduced allocation. The estimator gives $\Delta T_\mathrm{A}^* = 0.45$ K per direction (0.32 K combined), placing every leaf and isolated structure at $\geq 13\sigma$ in HCN via the M17 HCN/CO ratio[14] and a $\sim 3\times$ dense-gas deficit at 5σ, for a total of 2×10.75 hr $\times$ 1.4 (overhead) ≈ 30 hours (or ≈26 hours at 0.34 K with $7''$ spacing if the allocation is reduced).

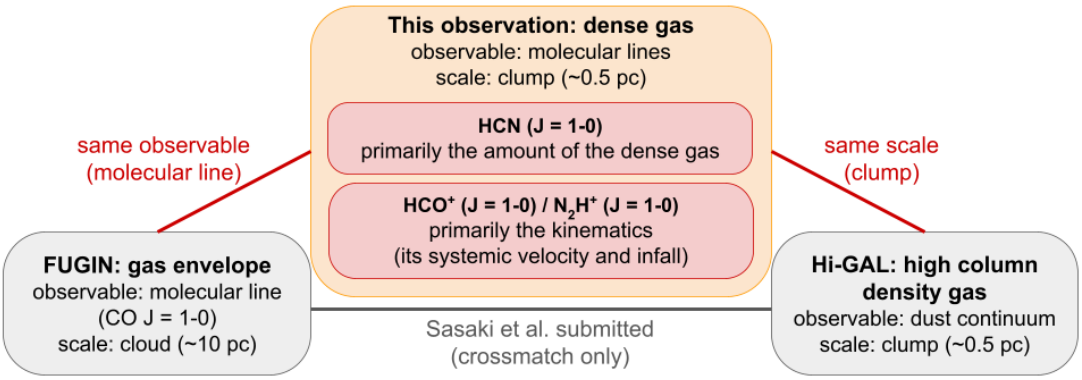

Figure 2: Relation of the proposed observation to the two existing datasets.

2 References

[1] Houlahan, P., & Scalo, J. 1992, *ApJ*, 393, 172
[2] Rosolowsky, E. W., et al. 2008, *ApJ*, 679, 1338
[3] Goodman, A. A., et al. 2009, *Nature*, 457, 63
[4] McKee, C. F., & Tan, J. C. 2003, *ApJ*, 585, 850
[5] Vázquez-Semadeni, E., et al. 2019, *MNRAS*, 490, 3061
[6] Umemoto, T., et al. 2017, *PASJ*, 69, 78
[7] Sasaki, K., et al. 2026, *PASJ*, submitted
[8] Elia, D., et al. 2021, *MNRAS*, 504, 2742
[9] Lada, C. J., et al. 2010, *ApJ*, 724, 687
[10] Wu, J., et al. 2005, *ApJL*, 635, L173
[11] Watanabe, Y., et al. 2017, *ApJ*, 845, 116
[12] Gao, Y., & Solomon, P. M. 2004, *ApJ*, 606, 271
[13] He, Y.-X., et al. 2015, *MNRAS*, 450, 1926
[14] Pérez-Beaupuits, J.P., et al. 2015, *A&A*, 583, A107